AD-A157 664

The Aerospace Spacecraft Charging Document

A. L. VAMPOLA, P. F. MIZERA,
H. C. KOONS, and J. F. FENNELL
Space Sciences Laboratory

D. F. HALL
Chemistry and Physics Laboratory
Laboratory Operations
The Aerospace Corporation
El Segundo, Calif. 90245

3 June 1985

APPROVED FOR PUBLIC RELEASE;
DISTRIBUTION UNLIMITED

Prepared for

SPACE DIVISION
AIR FORCE SYSTEMS COMMAND
Los Angeles Air Force Station
P.O Box 92960, Worldway Postal Center
Los Angeles, CA 90009-2960
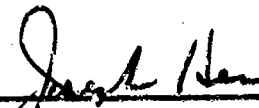
DTIC FILE COPY

85 .8 01 00

This report was submitted by The Aerospace Corporation, El Segundo, CA 90245, under Contract No. FO4701-83-C-0084 with the Space Division, P.O. Box 92960, Worldway Postal Center, Los Angeles, CA 90009. It was reviewed and approved for The Aerospace Corporation by H. R. Rugge, Director, Space Sciences Laboratory; and S. Feuerstein, Director, Chemistry and Physics Laboratory. Lieutenant Douglas R. Case, SD/YCM, was the project officer for the Mission-Oriented Investigation and Experimentation (MOIE) Program.

This report has been reviewed by the Public Affairs Office (PAS) and is releasable to the National Technical Information Service (NTIS). At NTIS, it will be available to the general public, including foreign nationals.

This technical report has been reviewed and is approved for publication. Publication of this report does not constitute Air Force approval of the report's findings or conclusions. It is published only for the exchange and stimulation of ideas.

DOUGLAS R. CASE, 1Lt, USAF
MOIE Project Officer
SD/YCM

JOSEPH HESS, GM-15
Director, AFSTC West Coast Office
AFSTC/WCO OL-AB

REPORT DOCUMENTATION PAGE	READ INSTRUCTIONS BEFORE COMPLETING FORM

1. REPORT NUMBER	2. GOVT ACCESSION NO.	3. RECIPIENT'S CATALOG NUMBER
SD-TR-85-26	AD-A157664	

4. TITLE (and Subtitle)	5. TYPE OF REPORT & PERIOD COVERED
The Aerospace Spacecraft Charging Document	
	6. PERFORMING ORG. REPORT NUMBER
	TR-0084A(5940-05)-10

7. AUTHOR(s)	8. CONTRACT OR GRANT NUMBER(s)
Alfred L. Vampola, Paul F. Mizera, Harry C. Koons, David F. Hall, and Joseph F. Fennell	F04701-83-C-0084

9. PERFORMING ORGANIZATION NAME AND ADDRESS	10. PROGRAM ELEMENT, PROJECT, TASK AREA & WORK UNIT NUMBERS
The Aerospace Corporation El Segundo, Calif. 90245	

11. CONTROLLING OFFICE NAME AND ADDRESS	12. REPORT DATE
Space Division	3 June 1985
Air Force Systems Command	13. NUMBER OF PAGES
Los Angeles, Calif. 90009-2960	43

14. MONITORING AGENCY NAME & ADDRESS(if different from Controlling Office)	15. SECURITY CLASS. (of this report)
	Unclassified
	15a. DECLASSIFICATION/DOWNGRADING SCHEDULE

16. DISTRIBUTION STATEMENT (of this Report)

Approved for public release; distribution unlimited.

17. DISTRIBUTION STATEMENT (of the abstract entered in Block 20, if different from Report)

18. SUPPLEMENTARY NOTES

19. KEY WORDS (Continue on reverse side if necessary and identify by block number)

Spacecraft Charging
Space Environment
SCATHA Program

20. ABSTRACT (Continue on reverse side if necessary and identify by block number)

This document presents basic information on spacecraft charging in the earth's magnetosphere, documents principal results from the engineering experiments on the USAF P78-2 satellite which was flown as part of the joint USAF-NASA spacecraft charging program (SCATHA), and makes recommendations for methods for alleviating the deleterious effects of spacecraft charging. It is intended as a primer for spacecraft designers and spacecraft program managers.

DD FORM 1473

CONTENTS

1

FIGURES

TABLES

Introduction

This document covers the topic of spacecraft charging in high, typically near-geosynchronous, orbit and is intended to provide spacecraft designers and program managers with elementary information on the spacecraft charging phenomenon. It includes the results of engineering experiments flown on a special test satellite, the USAF P78-2 which was part of the joint USAF-NASA Spacecraft Charging at High Altitudes (SCATHA) program, and makes a number of recommendations directed toward alleviating problems caused by spacecraft charging. Specific topics covered are: the spacecraft charing process; the geosynchronous altitude plasma environment; charging of surfaces; bulk charging; discharge pulse characteristics; and, contamination of surfaces due to charging. Information on the results of ground-based investigations of the SCATHA program was presented at three conferences on Spacecraft Charging Technology and was published as proceedings by NASA and the USAF under the following indices: (NASA) Conf. Pub. TMX 73537, 2071, and 2182; (USAF) AFGL-TR-77-0051, AFGL-TR-79-0082, and AFGL-TR-81-0270.

Summary

This section summarizes the main results presented in the chapters on the synchronous-orbit altitude environment, surface charging, bulk charging, environmentally-induced discharges, and charging-enhanced contamination.

Environment

Surface charging of spacecraft materials in the geosynchronous orbit environment is caused primarily by electrons with energies in the few keV (kiloelectron volt) to tens of keV range. The potentials reached during charging events depend on many additional factors, the most important being secondary-electron emission due to solar ultraviolet radiation and due to primary electrons and ions, and the density of the cold plasma which may supply a neutralizing current to a charged body. Differential potentials between different locations on a spacecraft are controlled by geometric considerations, material properties, and charging time-constants.

A severe environment, intended for use in modeling calculations, is presented in Chapter 2. In sunlight, the P78-2 satellite frame potential rose to -1600 volts relative to the plasma environment. Dielectric surface samples of Teflon and Kapton acquired differential potentials relative to the frame of -6400 volts and -1500 volts, respectively.

Bulk charging of spacecraft materials is caused primarily by electrons with energies of a few hundred keV to 1.5 MeV (megaelectron volts). These energetic electrons can penetrate thin shielding (spacecraft skin, cable shielding, etc.) and deposit charge in cables, circuit boards, and conductors. Depending on the fluence of the primary electrons and the conductivity of the dielectric, the material may experience a discharge which may couple into sensitive electronic circuits. In typical dielectrics, the breakdown may occur with fluences of the order of 10^{11} to 10^{12} e$^-$/cm^2. Electron fluxes with energies above a few hundred keV maximize at altitudes several earth radii below geosynchronous orbit following large magnetic storms. However, even at geosynchronous altitude, energetic electrons can alter electrical properties of dielectrics and influence differential charging effects.

Surface Charging

Differential charging near geosynchronous altitude depends on the local time, the altitude of the spacecraft, and the geomagnetic conditions at the time. Typically, the local-time distribution of charging begins a few hours before midnight and extends to the morning sector. At altitudes above geosynchronous, the probability of charging during disturbed magnetic conditions is a factor of two greater than during magnetically quiet times. At altitudes below geosynchronous, significant surface charging occurs only during disturbed magnetic conditions.

The electrical properties of dielectric materials can change significantly during exposure to the space environment. Therefore, laboratory simulations and satellite tests must be conducted using proper environmental parameters and lifetime tests should be considered. For example, the conductivity of Kapton increased orders of magnitude when exposed to solar radiation (see Chapter 3). Aging of Kapton thermal blankets in orbit may reduce a satellite's susceptibility to surface discharges.

The greatest surface charging stresses occur between dark and sunlit surfaces, between shadowed dielectrics and structure ground which is sunlit somewhere on the satellite, and during rapid changes in either the solar illumination of the satellite or the plasma environment. Shadowing of the satellite surfaces by motions of the satellite and projections from it can set up the conditions for surface charging.

An analytical function is specified for use as a severe near-geosynchronous orbit plasma environment. Dielectrics and satellite structure were observed to charge to greater than 1500 volts in this environment when shadowed.

Bulk Charging

Bulk charging near geosynchronous orbit altitude depends on the local time, the altitude of the spacecraft and the magnetic activity. Typically, bulk charging occurs at geosynchronous altitude and lower altitude hours to days after large magnetic storms. High energy electrons embed themselves within dielectrics and may build up potentials in excess of the breakdown potential of the material. Certain design approaches can reduce discharges

due to bulk charging. Shielding and grounding of cables and circuit boards are among these methods. Circuit susceptibility to spurious discharges can be reduced by reducing their sensitivity to low level pulses.

Discharges

Discharge pulses have been shown to occur during charging events on the P78-2 satellite in near-geosynchronous orbit. The frequencies of the Fourier components of these pulses are typically in the few to tens of megahertz region. Amplitudes can vary from a few tenths of a volt to tens of volts on a 50-ohm input. Arc-injection tests performed on the P78-2 satellite per MIL-STD 1541A were adequate to simulate most of the discharges that occurred in orbit, but not all of them. There is some evidence that larger pulses occurred on the P78-2 satellite after several years exposure to the space environment.

Contamination

Molecules emitted by the spacecraft can be ionized by solar radiation while still within the spacecraft plasma sheath and be reattracted to negatively charged surfaces. The more negative the potential on the surface, the higher the probability of contamination. Trying to control the potential of a spacecraft ground may increase the differential potential to adjacent dielectric surfaces and might even increase contamination buildup on some surfaces. Analysis of P78-2 data indicates that contamination rates are increased during periods of spacecraft charging.

Chapter 1 - Introduction to Spacecraft Charging

Anomalous behavior of satellite subsystems operating at geosynchronous orbit altitude (about 36,000 km) led to the speculation that low energy plasma (ionized positive and negative particles) could raise the potential of the vehicle relative to the plasma to such a level that electrostatic discharges on the vehicle could adversely affect logic systems (Garrett, 1981, and references therein). The necessary conditions appear to be a high flux of electrons in the tens of keV range heated during a magnetospheric substorm, with a very low cold plasma density. The cold plasma usually discharges the vehicle, provided the density is high enough.

The Spacecraft Charging at High Altitudes (SCATHA) program was initiated in the mid-1970s to provide: a) an understanding of the interaction between an object (spacecraft) immersed in a plasma (space environment); b) spacecraft materials which are not subject to charging or degradation in the space environment; c) proper laboratory simulations of the environment; and, d) in-situ measurements of engineering and science parameters. The P78-2 satellite was the test vehicle which obtained the in-situ measurements.

Differential Charging

The charging of a body in the space plasma depends on the current balance between many sources, including primary electrons and ions, secondary electron emission from surfaces due to impact by primaries, and ultraviolet radiation from the sun (Eq. 1, Chapter 2). Different materials on a spacecraft will charge to different voltage levels that depend on the material properties and the plasma parameters. For example, the energy at which secondary electron production coefficients become greater than or less than unity is much different for conductors than for insulators. Materials with different properties, adjacent to each other, can charge to different voltages and produce electrostatic discharges if the electric field gradient becomes too large. Insulators shadowed by the vehicle may charge differentially with respect to nearby vehicle frame which is "clamped" to the space plasma potential by secondary emission from an illuminated portion of the vehicle frame.

13

Bulk Charging

Intense fluxes of energetic electrons, when stopped in dielectrics such as cable insulators and circuit boards, can produce potentials which exceed the breakdown threshold in the dielectric if the rate at which charge is being deposited is large compared to the rate at which it bleeds off. When, and if, breakdown occurs, the energy of the discharge is coupled directly into the conductors involved in the discharge.

Electrostatic Discharges

When the electric field between two objects exceeds a critical value (about 10^6 volts/meter), a discharge can occur. However, transient electrical pulses observed in association with charging may be due to capacitive coupling effects rather than breakdown if the field gradient is below the critical value (Reagan et al., 1982). At times when large flux levels of energetic electrons are measured, internal redistribution of high field potentials can also discharge a material (Reagan et al., 1982). Discharge pulses measured on the P78-2 satellite had dominant frequencies from 5 to 32 MHz and peak amplitudes ranging from 0.08 to 30.1 volts across a 50-ohm input impedance (Koons, 1982).

Enhanced Contamination

Organic molecules outgassed from materials of spacecraft construction depart from the vehicle with thermal velocity. Eventually the molecules are converted to positive ions by interaction with solar UV photons or ambient electrons. A fraction of the total are ionized sufficiently close to the vehicle that they are electrostatically re-attracted to negatively charged surfaces (Cauffman, 1980; Clark and Hall, 1981).

Chapter 2 - The Geosynchronous Orbit Charging Environment

Introduction

A body immersed in a plasma will become negatively charged due to the fact that the electrons, which have a much smaller mass than the ions, have a much greater velocity than the ions and impact the body at a higher rate than the ions. Charging is limited by secondary electrons being emitted from the surface and being repelled by the negative potential, by ions being accelerated to the body by the potential, by the potential modifying the paths of incoming electrons, reducing the number that collide with the body, and, if the body is illuminated, by photoelectrons being emitted from the body. In space, the solar UV radiation is sufficiently intense that a body is normally a <u>few volts positive</u> with respect to the plasma (more photoelectrons are leaving the body than plasma electrons are arriving). Additionally, at lower altitudes (within a region called the "plasmasphere" which extends up to about 5 earth radii), the plasma has a dense (10^2 to 10^4 particles per cm^3) "cold" component which can supply sufficient ions or electrons to maintain the potential on a body close to the potential of the plasma.

At high altitudes, the cold plasma may at times be very tenuous (below 1 particle per cm^3) and unable to supply a neutralizing current to a body immersed in it. At these times, photoemission can charge a body to tens of volts positive with respect to the plasma. However, geomagnetic substorms heat plasma in the tail of the magnetosphere (and perhaps in the auroral regions) and inject the hot plasma into the region near geosynchronous altitudes. The hot plasma, with very high velocity electrons at substantial densities, can charge the body to high negative potentials in the absence of sunlight. Good correlations have been observed between levels of charging and electron fluences with energies of 20 keV or greater (Mullen and Gussenhoven, 1983).

Current Versus Potential

The potential of a surface on a spacecraft correlates with the integrated plasma electron current to the surface (Mizera, 1983). The potential of a surface changes so that in equilibrium, the net current to the surface is zero. That is,

$$J_{pe}-J_{pi}-J_{se}-J_{si}-J_{be}-J_{ph}=0 \qquad (1)$$

where

J_{pe} = incident plasma electron current

J_{pi} = incident plasma ion current

J_{se} = secondary electron current due to J_{pe}

J_{si} = secondary electron current due to J_{pi}

J_{be} = backscattered electron current due to J_{pe}

J_{ph} = photoelectron current

Each of these current contributions is a function of the surface potential relative to the plasma and to neighboring surfaces. Nominal values of J_{ph} are available (elsewhere in this chapter) and empirical estimates of J_{se}, J_{si} and J_{pe} have been made for satellite frames and some materials (DeForest, 1972; Feuerbacher and Fitton, 1972; Fredericks and Scarf, 1973; Grard et al., 1973; Grard, 1973). These parameters are contained in charging codes such as the NASCAP code (NASA Spacecraft Charging Analyzer Program) (Katz et al., 1979).

Since the distribution of the plasma electrons is controlled by the geomagnetic field, the potential of a surface will be modulated as it changes its orientation relative to the local magnetic field direction. This is usually a small effect which can be ignored to first order and an orientation-independent plasma distribution can be used.

The photoelectron current density is proportional to the cosine of the angle between the surface normal and the sun line. As a result, the spacecraft frame and material surface potentials will be modulated as the spacecraft changes its attitude relative to the sun. This can be a large effect and cannot be ignored. The largest electrical stresses often occur across the terminator (boundary between sunlight and shadow) of the spacecraft. During charging events, sunlit surfaces are usually near zero potential and dark surfaces are negatively charged. The potential difference is often greater than one kilovolt. This difference can lead to arcing across the terminator on insulating surfaces.

16

The nominal photoelectron current density for illumination of a material which has its surface normal parallel to the sun line is 1 na/cm^2. This number is relatively insensitive to material properties, varying by at most a factor of two from one material to another (Grard, 1973).

The plasma current density can be calculated as

$$J_p = \int v\, f_e(v)\, dv^3 - \int v\, f_i(v)\, dv^3 \qquad (2)$$

where v is the particle velocity and $f_e(v)$ and $f_i(v)$ are the electron and ion velocity distributions, respectively. Equation (2) ignores the secondary and backscatter electron current; which would reduce J_p. These latter currents are material-dependent. The particle velocity distribution is given by

$$f(v) = n_1[m/(2kT_1)]^{3/2} \exp(-mv^2/kT_1) + n_2[m/(2kT_2)]^{3/2} \exp(-mv^2/kT_2) \qquad (3)$$

where n is the number density (cm^{-3}) of the plasma electrons or ions, m is the effective mass (grams) of the electrons or ions, k is Boltzman's constant, T is the electron or ion "temperature" (keV), and the subscript index refers to the lower energy and higher energy components in a two-component plasma (the "cold" and "hot" plasmas mentioned previously).

Extreme Case Charging Environment

For the purposes of modeling spacecraft responses to the space plasma conditions, an extreme environment (from the point of view of causing spacecraft charging) is offered. This environment was the most extreme condition encountered during the first year of P78-2 operations and was one of the worst experienced during the entire mission. This environment is represented by a two-Maxwellian (Eq. 3) least-squares fit to data obtained by the P78-2 satellite during a charging event on 24 April 1979 (Mullen et al., 1981). The parameters for evaluating Eq. (3) are given in Table 1. Note that different parameters are furnished for particles travelling perpendicular to and parallel to the magnetic field lines.

The values for the particles 'perpendicular' to the magnetic field should be used in analysis unless the satellite orientation relative to the magnetic field vector is known. The data used to obtain these coefficients and the

17

fits to these data are shown in Fig. 1. The curves are the two Maxwellian approximations for the directions perpendicular (solid curve) and parallel (dashed curve) to the earth's magnetic field vector.

	n_1 (cm^{-3})	n_2 (cm^{-3})	T_1 (keV)	T_2 (keV)
Ions				
Perpendicular	1.1	1.3	0.3	28.2
Parallel	1.6	0.6	0.3	26.0
Electrons				
Perpendicular	0.2	2.3	0.4	24.8
Parallel	0.2	0.6	0.4	24.0

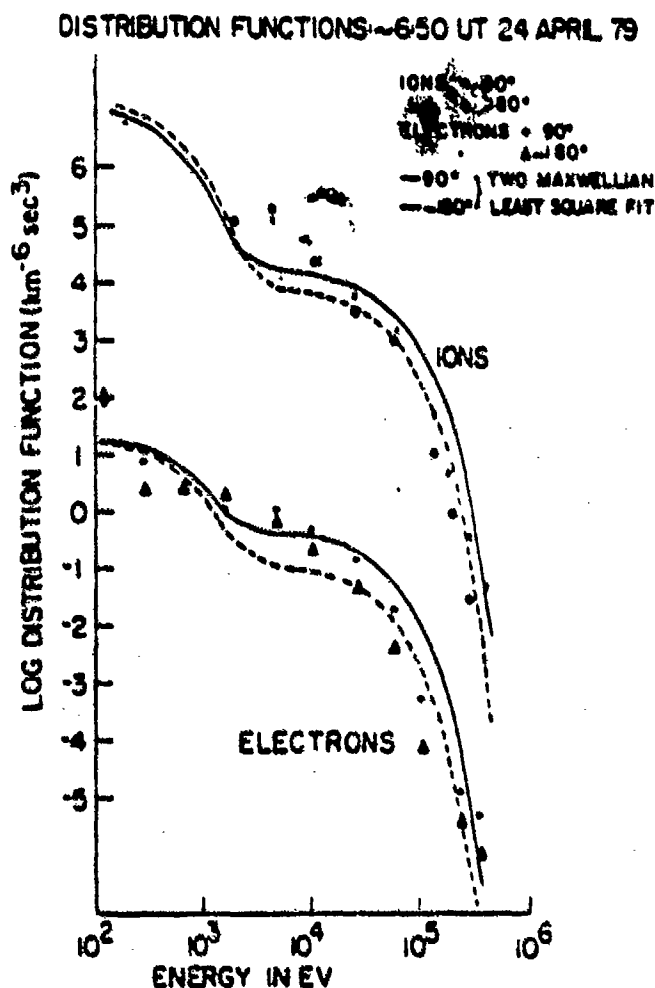Table 1. Two-Maxwellian parameters for an 'Extreme' plasma environment.

Figure 1. Data (symbols) and calculated fits (curves) for the extreme plasma environment encountered by the P78-2 satellite near geosynchronous orbit on 24 April 1979.

Sunlight Versus Shadow Charging

The environment defined in Table 1, combined with the zero-net-charge condition of Eq. (1), the estimate on photocurrent and the calculated plasma current using Eq. (2), produces an estimated charging conditions as follows: sunlit satellite frame-to-plasma potential of a few hundred volts; shadowed area-to-plasma potential greater than 10 kilovolts. A maximum potential of 16 kV occurred on the P78-2 when exposed to this environment (Mullen et al., 1981). Dielectrics would be expected to charge to a few kilovolts relative to spacecraft ground and relative to each other on a shadowed satellite. In sunlight, a few kilovolt potential difference would exist between shadowed dielectrics and the sunlit materials or exposed structure ground.

The P78-2 experiment complement included a Satellite Surface Potential Monitor (see Chapter 3). Table 2 lists several materials measured by the SSPM and the levels to which they charged during the 24 April 1979 charging event.

Sample	Potential[*]
Quartz Fabric	-3800 V
Silvered Teflon	-6400 V
Aluminum Kapton	-1500 V

[*]Surface potential relative to satellite ground. The satellite ground was at -1600 V relative to the plasma.

Table 2. SSPM potentials measured during the 24 April 1979 charging event.

High voltage stress associated with breakdown and arcing occurs most often during rapid changes in conditions such as a sudden change in the environment or a sudden shadowing of parts or all of the spacecraft. Periodic self-shadowing on a rotating spacecraft can lead to periodic discharges (Mizera et al., 1981).

The Satellite Surface Potential Monitor

One of the instruments flown on the P78-2 satellites for in-situ measurements in the spacecraft charging program was a Satellite Surface Potential Monitor (SSPM). The measurement technique is shown in Fig. 2. A sample of material for which the surface potential is to be monitored is mounted on a sheet of dielectric material (fiberglass-epoxy) with a conducting layer (typically evaporated aluminum on the back of the sample) between them. The dielectric sheet is mounted in a conducting frame. The conductive layer is isolated from the frame but is connected to a high-impedance current meter. At the center of the sample (typically 10 cm square), the back side of the sample is viewed over an area of about 0.4 cm diameter by a vibrating-reed electrometer. The conductive layer is removed over this area. Simultaneous measurements of the surface potential and the total current to the sample were made. Laboratory calibrations were made to obtain conversion coefficients for relating back-side measurements to the actual surface potential. Potential measurements were referenced to the frame potential. These in turn were referenced to a measurement of the frame potential to a gold-plated circumferential strip on the vehicle which, whenever the satellite was in sunlight, had some portion illuminated and therefore was clamped to a low level by photo-emission. Table 3 lists the samples monitored by the SSPM, gives the mnemonic for the sample, and shows the location on the satellite. 'Bellyband' refers to a central area of the cylindrical body which was free of solar-cells.
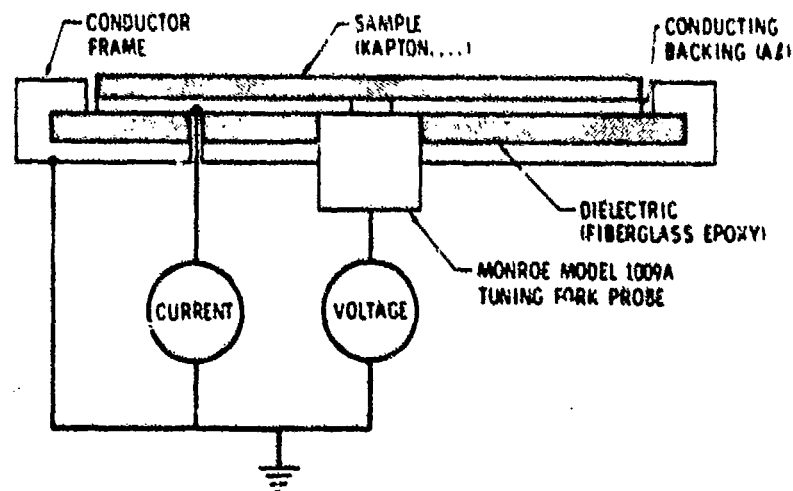
Figure 2. The P78-2 Satellite Surface Potential Monitor technique.

Sensor	Location	Sample	Material
SSPM-1	Bellyband ⊥ to spin axis	1	Kapton
		2	Optical Solar Reflector[a]
		3	Optical Solar Reflector
		4	Gold-plated Magnesium
SSPM-2[b]	Bellyband 180° from SSPM-1	1	Kapton[c]
		2	Kapton
		3	Reference Band (high gain amp)
		4	Reference Band (low gain amp)
SSPM-3	Bottom of S/C 90° from sun	1	Kapton
		2	Teflon
		3	Quartz Fabric
		4	Gold-flashed Kapton[d]

Notes: a) Grounded to frame
        b) 30 cm square Kapton sample
        c) Hole through Kapton over sensor

Table 3. Satellite Surface Potential Monitor samples and locations.

Probabilities of Charging

Since the P78-2 satellite was spinning, the SSPM charging levels typically represented non-equilibrium values when a sample entered the shadow of the satellite. Equilibrium values may have been a factor of two higher. Figure 3 shows the percent probabilities of Kapton charging greater than -100 volts and -500 volts during solar illumination and quiet geomagnetic conditions. These data are for periods with K_p less than or equal to 2+. K_p is a planetary index of high latitude magnetic activity. The results are grouped into high and low altitudes (relative to geosynchronous orbit altitude) and into 3-hr local time intervals. L = 6.6 R_e (earth radii) is a geosynchronous orbit at the equator. The P78-2 orbit was elliptical and extended about one earth-

22

radius above and below geosynchronous orbit altitude. In Figure 3, Kapton-1,2 refers to the Kapton samples on the SSPM-1,2; M indicates midnight; MLT is the magnetic local time (the local time at which the magnetic field line crosses the equator). The Kapton-2 sample was four times as large as the Kapton-1 sample. The slight differences in charging probabilities may be due to differences in the way they approached equilibrium or may have been influenced differently by other surfaces in their vicinities charging differently.
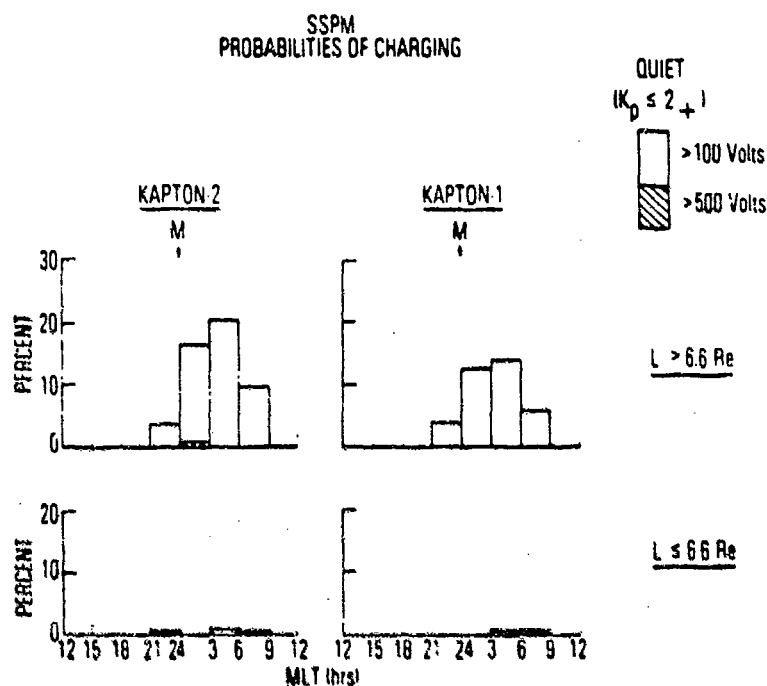
Figure 3. Probabilities of Kapton charging to levels in excess of -100 volts and -500 volts in sunlight during quiet magnetic conditions.

Figure 4 shows data similar to those of Figure 3 but for disturbed magnetic conditions. These data show clearly that differential surface charging is strongly dependent on local time, altitude, and magnetic conditions.

Figure 5 shows data similar to Figure 4 for two other samples on the SSPM. Only data for disturbed magnetic conditions are shown because these two samples, the gold-plated magnesium and optical solar reflecting tiles (OSR), do not charge to high values. The OSR tiles were bonded with conductive epoxy. These figures illustrate the importance of material properties and configuration in determining the charging behavior in space.

23

Figure 4. Data similar to Fig. 3 but for disturbed magnetic conditions.
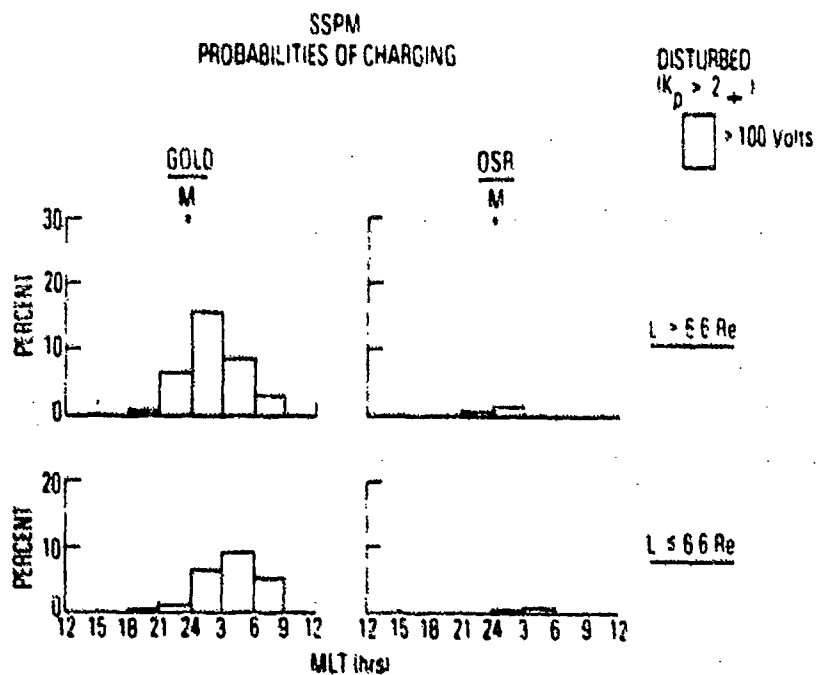
Figure 5. Charging probabilities of Gold-plated Magnesium and Optical Solar
Reflectors in sunlight during disturbed magnetic conditions.

24

Near-Geosynchronous Charging

Figure 6 shows the percent probability of charging for a typical insulating material (Kapton) during geomagnetically disturbed conditions near geosynchronous orbit altitude. The data are plotted as a function of magnetic local time which for this data can be assumed to be equivalent to local time. The important features to be noted in Figure 6 are: high level charging occurs primarily a few hours before local midnight; the highest frequency of low-level charging occurs some 5 hours past local midnight.

SSPM
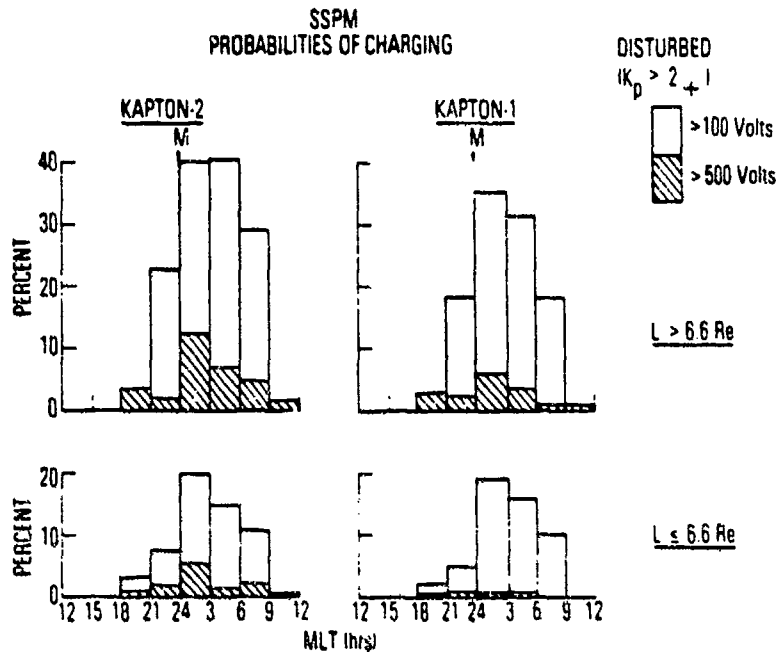NEAR-GEOSYNCHRONOUS CHARGING
(Disturbed Times)
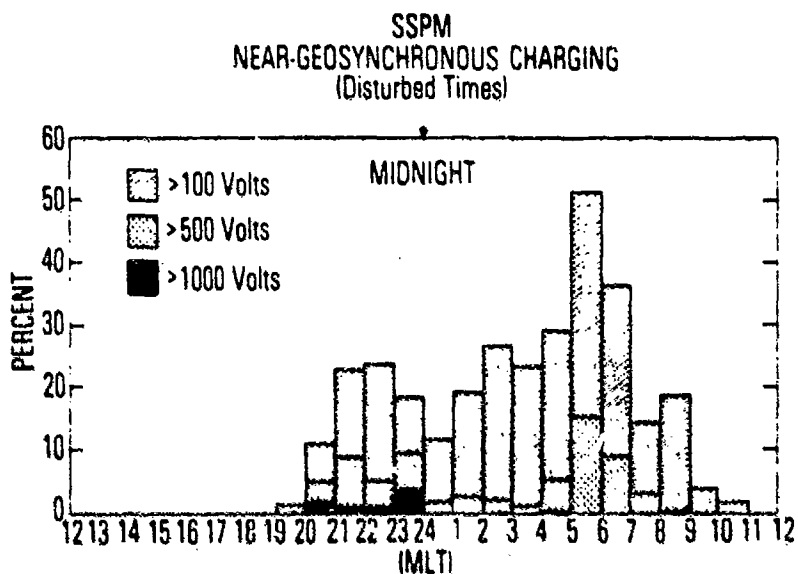
Figure 6. Probability of charging near geosynchronous orbit during magnetically-disturbed conditions.

Figure 7 shows the complete coverage of dielectric charging as a function of local time and L (equivalent to earth-radii at the equator). The outer curve delineates the highest altitude coverage by the P78-2, the circle at L = 6.6 represents geosynchronous orbit, and the inner curve represents the lowest altitude coverage. There are three contour categories in Fig. 7: The solid line bounds the 10% probability of charging to greater than -100 volts; the dashed curve outlines the region where the -100 volt probability is greater than 50%; the cross-hatched area is the region where the probability for charging to greater than -1000 volts is 10%. Although there are some regions (denoted by grey in Fig. 7) where the total time spent was less than 1.5 hours during the 9-month period represented in Figure 7, the overall charging proba-

bility contours illustrate the regions where a vehicle can experience differential charging.

DISTURBED-TIME SSPM CHARGING
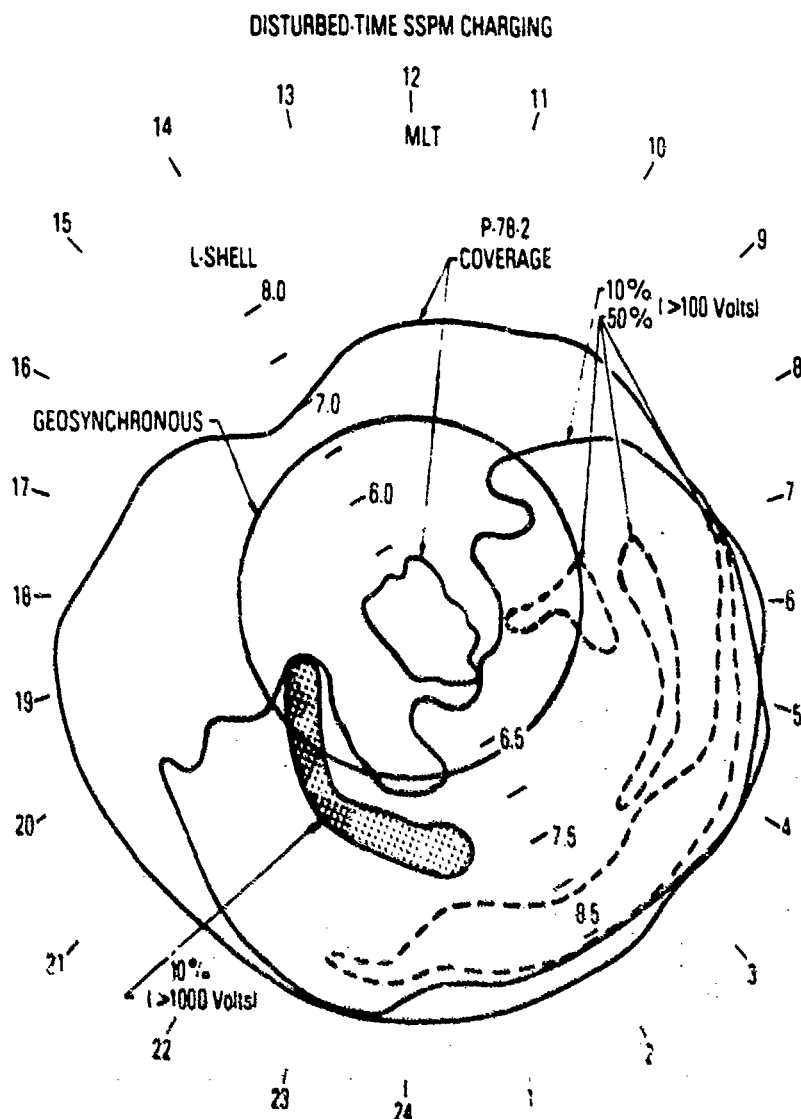
Figure 7. Contour plot of the probability of Kapton charging to greater than -100 and greater than -1000 volts as a function of altitude and local time during magnetically-disturbed conditions.

Changes in the Properties of Materials

Data from the SSPM experiment showed dramatic and significant changes in the electrical properties over a period of months in the space environment. Figure 8 represents a plot of the ratio of the potential measured on Kapton referenced to the potential on the gold-plated magnesium for a period of 9 months after launch. Data were obtained during charging events. An exponential decrease in resistivity of the Kapton sample was observed such that it

26

decreased by 1/e every 87 days. The change is a result of exposure to sunlight in vacuum. These results have been verified in the laboratory under controlled conditions (Leung et al., 1982). There is some evidence that after long exposure in space (several years), the resistivity begins to increase again.
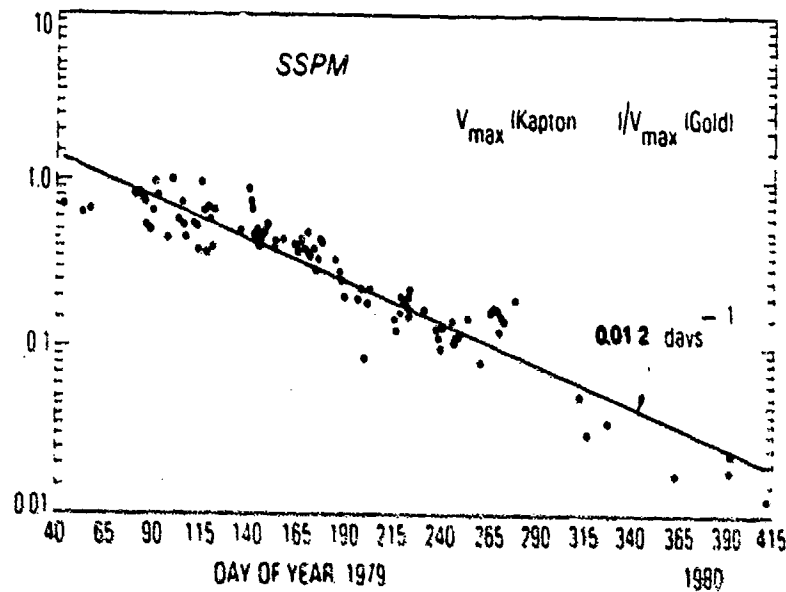
Figure 8. Ratio of the potential measured on Kapton to the potential measured on gold-plated magnesium during charging events.

An apparent "bulk" potential on the Teflon sample was observed. Figure 9 shows the potential measured on the Teflon sample as a function of time. These daily values are not due to surface charging but probably result from a buildup of charge due to energetic electrons embedding themselves in the bulk of the sample (see Chapter 4). Some of the daily variations seen in Figure 9 are due to partial discharging of the sample due to grazing-incident solar UV.

TEFLON

NO
DATA

NEGATIVE VOLTAGE

4000
3800
3600
3400
3200
3000
2800
2600
2400
2200
2000
1800
1600
1400
1200
1000
800
600
400
200

30 50 70 90 110 130 150 170 190 210 230 250 270
DAY OF YEAR 1979
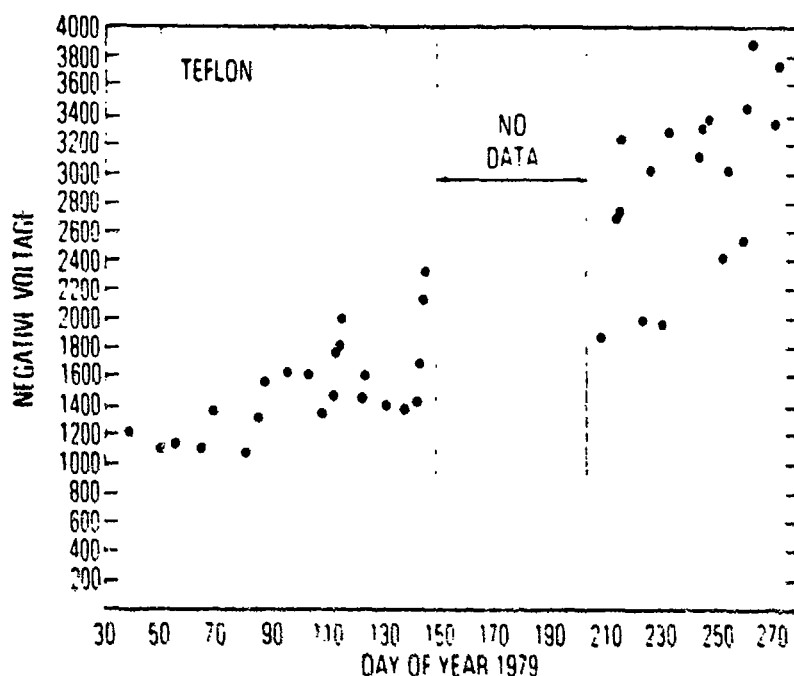
Figure 9. Potential measured on Teflon showing a time-dependent increase.
The effect is probably due to a buildup of charge embedded in the
sample.

Summary

Differential charging occurs aboard high-altitude satellites when materials isolated from frame potential are shadowed from solar UV. When a spacecraft enters the earth's shadow, differential charging can still occur because different materials have different secondary electron emission coefficients. Depending upon the charging time constants of different surfaces, the maximum electrical stress may occur at these times. Differential charging depends strongly on local time, altitude, and magnetic activity.

Dielectric material properties can change in the space environment. It is impossible to predict long-term charging behavior unless long-term material properties in the space environment are known. A method of determining these changes in properties is to monitor witness samples of critical materials either aboard a space vehicle or under proper laboratory conditions. Improper modeling of the space environment for laboratory simulations can lead to large errors in predictions of on-orbit materials performance. For example, earlier laboratory simulations predicted the SSPM OSR sample would charge significantly higher than was actually observed in space. Conversely, the SSPM quartz

28

fabric sample charged to low values in laboratory simulations while values an order of magnitude (or more) higher were commonly observed in the space environment.

Introduction

In certain regions of the earth's magnetosphere, primarily between L = 3 and L = 5.5 but extending out past geosynchronous orbit altitudes after large magnetic storms, frequently sufficient fluxes of energetic electrons are present to produce an effect known as "bulk charging". The mechanism is shown schematically in Figure 10. Energetic electrons, with energies in the range of 300 keV and higher, penetrate through thick dielectrics such as cable insulators or circuit boards. If the rate at which particles are incident exceeds the rate at which embedded charge can leak out of the dielectric, the embedded charge and its image charges on the cable, circuit board, or nearby conductors may produce a potential in excess of the breakdown potential of the dielectric in that particular geometry. The resultant breakdown produces a fast pulse on devices connected to the cable or mounted on the circuit board.

- ENERGETIC ELECTRONS CHARGE UP DIELECTRIC

- IMAGE CHARGES ON CONDUCTORS BALANCE TRAPPED CHARGE

- DIELECTRIC BREAKS DOWN, RESULTING IN FAST PULSE ON DEVICES CONNECTED TO CABLE
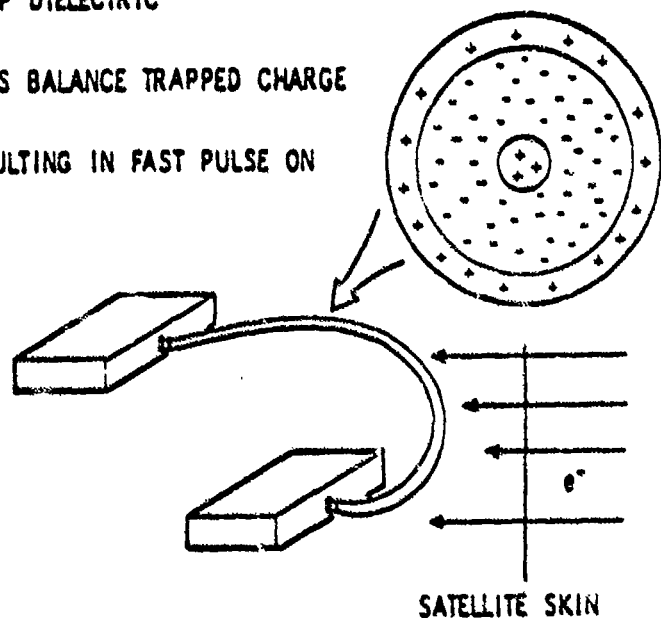
SATELLITE SKIN

Figure 10. The "Bulk Charging" mechanism.

The rise and fall times of such pulses are of the order of tens of nano-seconds. The energy content of the pulse depends on the capacitance of the geometry being discharged, but is usually of the order of a few nanojoules or less. Pulse lengths up to 100 nanoseconds may be observed. The source is a high impedance current source and may produce peak voltages in the tens to hundreds of volts on high impedance inputs. The total fluence required to build up potentials to the breakdown value depends on the flux intensity and the conductivity of the dielectric, but in typical dielectrics is of the order of 10^{11} to 10^{12} electrons per square centimeter in a time short compared with the bleed-off time constant of the dielectric.

Energetic Charged Particle Environment

The rate at which charge is deposited depends upon the incident charged particle flux and the amount of matter the particles have to penetrate to get to the dielectric. As a general rule, electrons with energies below 300 keV do not have enough energy to be a problem (they are stopped by 20 mils of aluminum or equivalent mass thickness) and fluxes above 1500 keV are always too low in the natural environment to produce the necessary potentials. The particle flux is variable and depends on energy, location in the magnetosphere, and time. Geomagnetic activity increases the flux levels and they remain high for some time after the geomagnetic activity subsides. Usually, after a major magnetic storm, high levels of energetic electrons are seen immediately at altitudes equivalent to L = 3 to 4. Within a day or two afterwards, these energetic electrons diffuse out to geosynchronous altitudes and may remain at elevated levels for several days. Models of the average energetic charged particle environment are issued by the National Space Science Data Center, World Data Center-A, Goddard Space Flight Center, MD 20771.

The maximum electron flux that may be present at a given point in space is not known, but Table 4 presents probable maxima as a function of threshold energy and L-shell (where L corresponds approximately to the distance, in earth radii, from the center of the earth to the point at which the magnetic field line on which a particle is trapped crosses the geomagnetic equator). Fluxes are given in units of e^-/cm^2-sec above threshold energy. Fluxes as high as these are observed perhaps once or twice per year. Typical peak fluxes are an order of magnitude lower.

Threshold Energy MeV	Geocentric Distance (R_e)				
	L=4.0	L=4.5	L=5.0	L=6.0	L=6.6
0.5	6×10^8	4×10^8	2×10^8	1×10^8	5×10^7
1.0	1×10^8	6×10^7	3×10^7	1×10^7	5×10^6
1.5	4×10^6	2×10^6	1×10^6	5×10^5	2×10^5

Table 4. Peak integral electron fluxes as a function of energy threshold and altitude.

Increased Probability of Bulk-Charging Discharge

Certain conditions are likely to increase the probability of a bulk charging discharge or coupling of energy from such a discharge into nearby circuitry. Such conditions are: a) exposure of bare cables or circuit boards to the space environment; b) large areas of metallization on circuit boards left ungrounded; and c) spare conductors in cables left unterminated at both ends.

The exposure of cables, circuit boards, or other dielectrics which are intimately connected to electronic circuitry to the space environment permits a much larger fluence of particles to impinge upon the dielectric with sufficient energy to produce a bulk-charging effect. The energy spectrum shows a large decrease in number with increasing energy, typically decreasing a factor of ten to thirty with an increase of a factor of three in energy. Therefore, shielding which eliminates all electrons below about 1 MeV should provide protection against even the largest fluxes observed in the natural earth environment. Smaller amounts of shielding, which stop all electrons with energies below 350 keV, should be effective against all but the largest flux events. A 1 MeV electron will be stopped by 0.5 grams/cm^2 of material. Lesser amounts of shielding will stop lower energy electrons but will also degrade electrons which initially have their energy in the 500 keV to 1 MeV range and reduce their effectiveness in producing bulk charging. Most spacecraft have sufficient mass in their external panels, solar cells, thermal blankets, etc. that no additional shielding is necessary for circuit boards and cables contained within the body of the spacecraft.

33

Large a* as of ungrounded metallization or unterminated conductors in cables act as collection points for migrating charges and increase the capacitance of the volume that can be discharged in a single breakdown. The magnitude of the pulse produced in discharges which include such elements is therefore much higher and is more likely to produce spurious responses or damage in circuit elements into which they couple.

Circuit designs can contribute to the susceptibility to or damage by bulk charging discharges. These include: a) coupling of discharge energy into the circuit; b) susceptibility of the circuit to pulses of the type generated in bulk charging discharges; and c) circuit elements with very low damage thresholds (e.g., unprotected high input impedance circuits).

Recommendations

Low-level high-speed circuitry should be kept well isolated from elements which may be susceptible to bulk charging. Long signal leads, especially those which exit the subsystem enclosure, should be avoided. Cables between well-shielded enclosures with low-level circuitry should carry only high-level signals. Signal conditioning should be used to eliminate responses to the fast low-level pulses characteristic of bulk charging discharges. Small circuit elements which might be damaged by nanojoule energy levels should be eliminated or should be protected by devices with sufficient response time and capability of handling pulses of either polarity originating in a high impedance current source.

Summary

Bulk charging is caused by large fluences of energetic electrons impinging upon thick dielectrics and embedding within the bulk of the dielectric, building up a potential. Subsequent discharges produce very fast pulses, typically less than 100 nanoseconds duration, with the characteristics of a high impedance current source. Problems due to this phenomenon can be alleviated by reducing the number of particles with sufficient energy to penetrate and embed within the dielectric (e.g., shielding), by design geometries which reduce the volume of the region which discharges (thereby reducing the size of the discharge pulse), or by reducing the susceptibility of the individual circuit elements to disruption by small signals.

Chapter 5 - Discharges

Discharge pulses were detected by the Pulse Analyzer and the Transient Pulse Monitor flown on the P78-2 satellite. Many pulses were detected during electron and ion beam operations (which were an attempt to control the potential of the satellite with respect to the plasma). A few pulses were observed due to natural charging events. Of the 550 days of data processed, the pulse analyzer detected 77 pulses on 35 different days that can be attributed to natural discharges.

The P78-2 Pulse Analyzer

There were two discharge monitors making in-situ measurements on the P78-2 satellite. One, the Transient Pulse Monitor, measured the peak amplitude and the area under an amplitude-vs-time curve for pulses observed on various inputs. The Pulse Analyzer, shown in Figure 11, measured the shape of electromagnetic pulses in the time domain from 7 ns to 3.7 ms. The Pulse Analyzer used four sensors: S0, an external short dipole antenna at the end of a 2-meter boom; S1, a loop antenna around one of two redundant space vehicle Command Distribution Units; S2, a wire along the outside of a 'typical' space vehicle cable bundle; and S3, a digital command line from the CDU to the Pulse Analyzer.
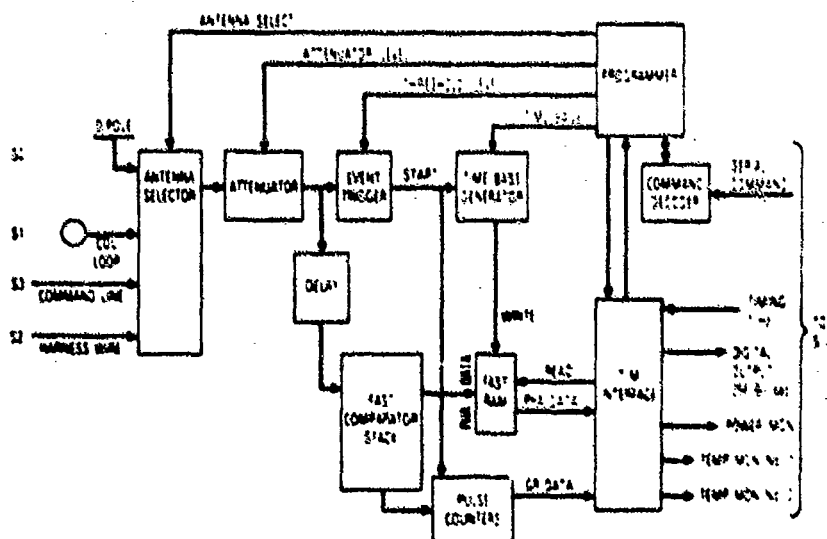

Figure 11. Schematic representation of the Pulse Analyzer on the P78-2.

For the 550 days of orbital data analyzed for the Pulse Analyzer, a total of 6381 pulses were observed. Of these, 4016 were transients due to normal operation of the vehicle. An additional 2288 pulses were observed during operations of electron and ion beam systems intended to control the potential of the vehicle relative to the space plasma. All of these pulses are thought to be due to discharges on the vehicle due to differential potentials set up by the operation of the beams. A total of 77 pulses, occurring on 35 separate days, are identified as being due to surface or bulk charging induced by the space environment. Table 5 lists the individual natural discharges, giving the date, time, local time, altitude (in earth radii), and the amplitude of the pulse. When the potential on the Kapton sample on the SSPM (Chapter 3) was known, it is listed in the last column.

NUM	DATE	UT	LT	Re	VOLTS	CHARGE		NUM	DATE	UT	LT	Re	VOLTS	CHARGE
1	79/03/28	59851	23.8	6.3	0.69	-1735		40	81/04/01	34920	1.3	6.5	2.80	
2	79/03/28	62088	0.4	6.5	0.35	-1689		41	81/04/01	35512	1.4	6.6	11.20	
3	79/04/14	39940	0.2	6.7	0.09	-400		42	81/04/22	3027	0.0	6.5	2.80	-883
4	79/04/18	82767	10.8	6.3	0.18	None		43	81/04/23	4016	0.1	6.6	11.20	-308
5	79/04/30	25616	1.2	7.4	0.18	-840		44	81/04/23	4150	0.1	6.6	11.20	-655
6	79/05/26	2641	2.6	7.8	0.35	-1098		45	81/10/08	72375	23.9	6.5	0.69	
7	79/05/26	2756	2.7	7.8	0.35	-1049		46	82/04/08	76284	11.5	6.7	0.18	
8	79/05/26	2929	2.7	7.8	0.35	-1074		47	82/09/22	27278	4.9	5.6	2.80	
9	79/05/26	3158	2.7	7.8	0.35	-1061		48	82/09/22	27244	4.9	5.6	0.69	
10	79/05/26	3287	2.8	7.8	0.69	-1012		49	82/09/22	27300	5.1	5.6	5.60	
11	79/05/26	3444	2.8	7.8	0.35	-1081		50	82/09/22	27359	5.1	5.6	2.30	
12	79/08/09	2095	2.3	6.7	0.35	-200		51	83/03/28	63473	6.2	7.7	0.09	
13	79/09/18	35981	1.5	6.2	0.69	-300		52	83/09/21	10766	0.3	7.0	0.69	
14	80/01/24	3082	12.2	5.4	0.35	None		53	83/09/23	48486	14.3	6.4	0.18	
15	80/03/24	41400	22.4	5.7	0.18			54	82/09/26	34779	10.9	5.6	0.09	
16	80/03/28	1508	9.3	6.9	0.35			55	82/09/27	59780	9.3	5.4	0.18	
17	80/03/28	1894	9.5	6.9	0.18			56	82/09/28	3072	0.4	6.8	0.69	
18	80/03/28	2437	9.6	6.9	0.18			57	83/09/28	3112	0.4	6.8	0.35	
19	80/03/28	3879	9.7	6.8	0.18			58	83/09/28	3147	0.4	6.8	1.40	
20	80/04/16	22281	0.5	7.2	0.69			59	83/09/28	3177	0.4	6.8	0.18	
21	80/04/13	4322	14.0	5.3	0.05	None		60	83/09/28	3213	0.4	6.8	0.69	
22	80/04/13	6750	15.0	5.6	0.18	None		61	83/09/28	3258	0.4	6.8	1.40	
23	80/04/14	6400	15.0	5.4	0.69	None		62	83/09/28	3302	0.6	6.9	0.69	
24	80/04/14	9770	16.7	5.6	0.09	None		63	83/09/28	3354	0.6	6.8	0.69	
25	80/04/18	10722	18.8	6.1	0.05			64	83/09/28	3433	0.6	6.8	2.80	
26	80/04/18	79850	12.8	5.3	0.09			65	83/09/28	3696	0.6	6.8	2.80	
27	80/04/19	74779	11.0	5.3	0.18			66	83/09/28	28315	9.5	5.4	0.02	
28	80/04/19	79964	13.3	5.3	0.02			67	83/09/28	73043	12.0	5.8	0.05	
29	80/04/20	20132	21.6	7.2	0.35			68	83/09/29	15817	4.6	5.6	0.05	
30	80/10/18	69734	1.6	5.7	0.35			69	83/09/29	19340	6.0	5.4	0.05	
31	80/10/18	70021	1.8	5.7	0.18			70	83/09/29	29586	10.3	5.3	0.09	
32	81/03/09	920	6.8	7.7	0.18			71	83/09/29	34709	12.3	5.9	0.35	
33	81/03/13	83258	23.8	5.8	0.35			72	83/09/30	10282	3.1	5.3	0.18	
34	81/03/13	83262	23.8	5.8	0.35			73	83/09/30	24108	8.3	5.4	0.35	
35	81/03/13	83263	23.8	5.8	0.35			74	83/09/30	28576	10.3	5.3	0.18	
36	81/03/21	6518	10.8	7.1	0.35			75	83/09/30	29520	10.7	5.6	0.02	
37	81/03/30	46222	2.5	7.2	0.35			76	83/09/30	63857	19.2	6.3	0.18	
38	81/03/31	35005	1.0	6.4	0.18			77	83/10/04	78055	0.0	0.0	0.18	
39	81/04/01	34568	1.1	6.5	11.20									

Table 5. Summary of natural discharges detected by the Pulse Analyzer on the P78-2 satellite.

Pulse Description

Figure 12 shows three typical severe waveforms of discharge pulses measured by the Pulse Analyzer on April 23, 1981.
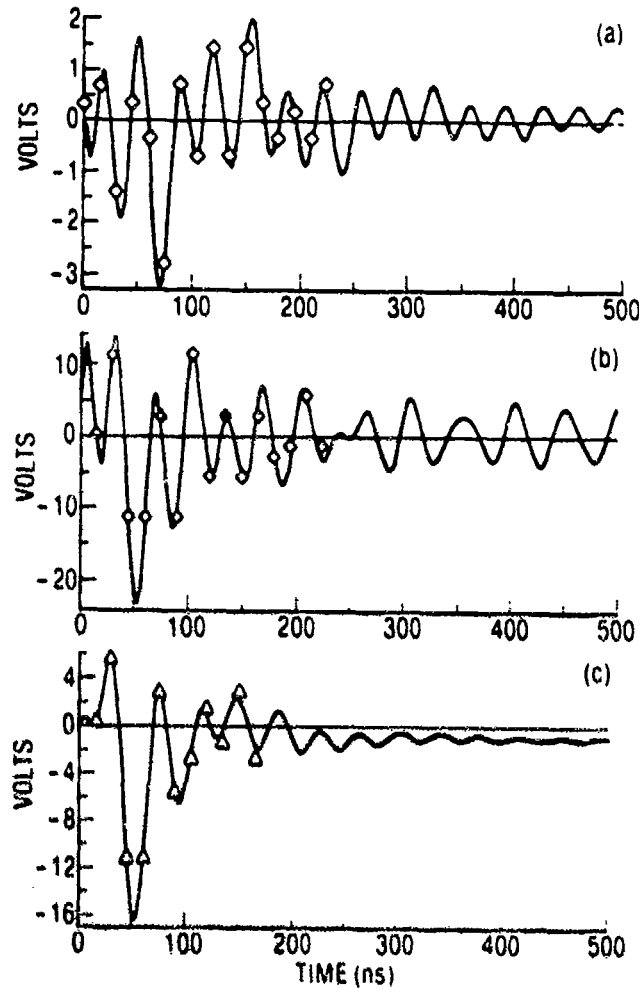

Figure 12. Fitted waveforms for three pulses measured by the Pulse Analyzer on April 23, 1981.

The actual voltage vs time data points were fit with the functional form:

$$V = V_0 + V_e e^{-k_e t} + \sum_i V_i e^{-k_i t} \cos(2\pi f_i t - \theta_i) \tag{4}$$

Table 6 shows the parameters used to fit the data for the pulses shown in Figure 12. For all natural discharge pulses, the dominant frequencies ranged from 5 to 32 MHz and amplitudes ranged from 0.08 to 30.1 volts. Prior to launch, the P78-2 was subjected to the MIL-STD-1541 Electrostatic Discharge Test. Figure 13 presents a histogram of the amplitudes of those test discharges. For comparison purposes, Figure 14 presents a similar histogram of the natural discharges listed in Table 5.

37

Date	UT sec.	Sensor	i	Freq. MHz (f_i)	Amplt. Volts (V_i, V_e)	Damp. 1/ns (k_i, k_e)	Phase deg. (ϑ_i)
4/23/81	3023	CDU loop	0	0	.06	0	0
			1	6.2	1.69	.0077	32
			2	17.8	1.69	.0087	58
			3	29.5	2.2	.005	153
4/23/81	4016	Harness wire	0	0	.18	0	0
			e	0	15.8	.027	0
			1	11.8	30.1	.022	-89
			2	20.7	2.6	-.00097	226
			3	29.7	19.0	.0077	-27
4/23/81	4150	Dipole	0	0	.49	0	0
			1	5.4	11.3	0.14	58
			2	18.0	16.8	.0204	215
			3	26.3	9.1	.01	20

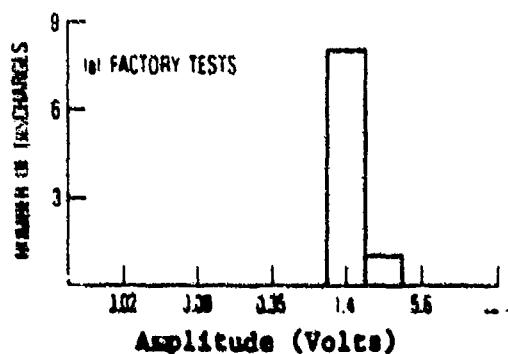Table 6. Natural discharge fitting parameters.

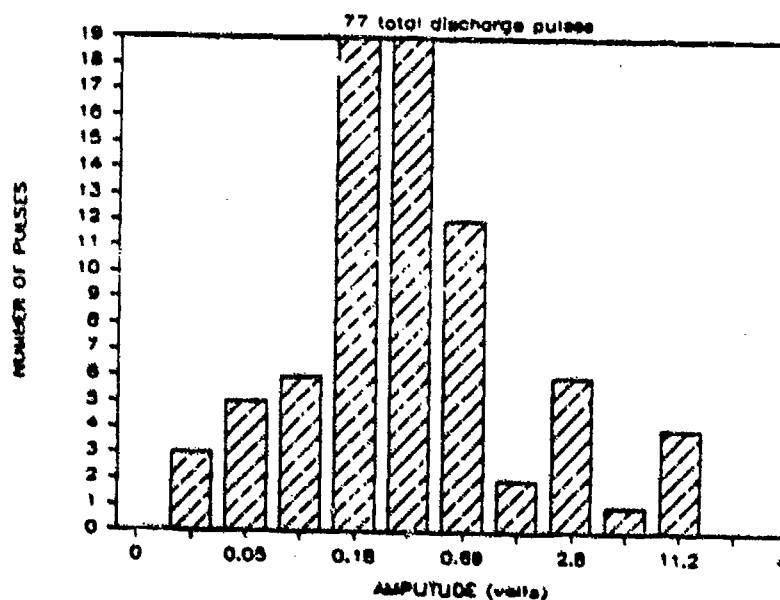Figure 13. MIL-STD 1541 test pulse distribution

Figure 14. Natural pulse amplitude distribution.

Since there is a difference in the mechanism of surface charging and bulk charging, the natural pulse amplitude distribution has been further sorted into surface and bulk charging distributions. Figures 15 and 16 show these amplitude distributions for surface and bulk charging, respectively.
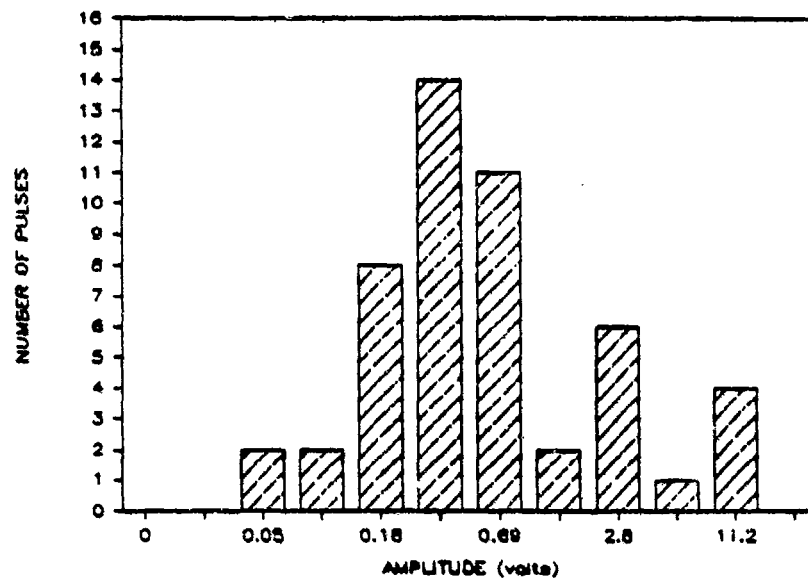
38

Figure 15. Pulse amplitude distribution for discharges attributed to surface charging.

The two primary points to be noted about these distributions is that the bulk charging pulses are much smaller than the surface charging pulses (but are much larger on the actual cables or other dielectrics where the discharges occur), and that some of the surface charging pulses far exceed the MIL-STD-1541 test pulses.
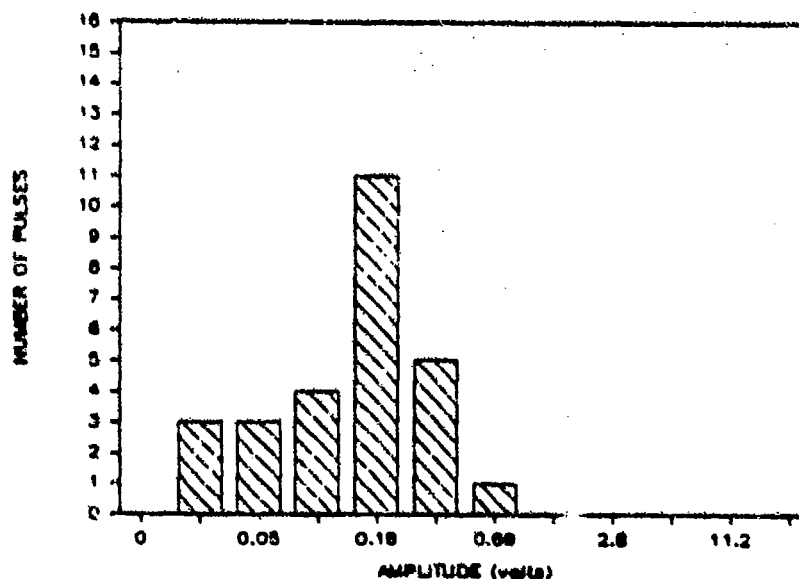

Figure 16. Pulse amplitude distribution for discharges attributed to bulk charging.

Morphology of Pulses

The location in local time and altitude (in units of earth radii) of the pulses shown in Fig. 14 is plotted in Figure 17. SYNC indicates the geosynchronous orbit altitude. Typically, pulses observed in the post-midnight sector and at higher altitudes were associated with surface charging. Those pulses not associated with surface charging events occurred in the late morning and afternoon time sectors and have been shown to be associated with large magnetic storms and increases in the flux of very energetic electrons. They are considered to be due to bulk charging.
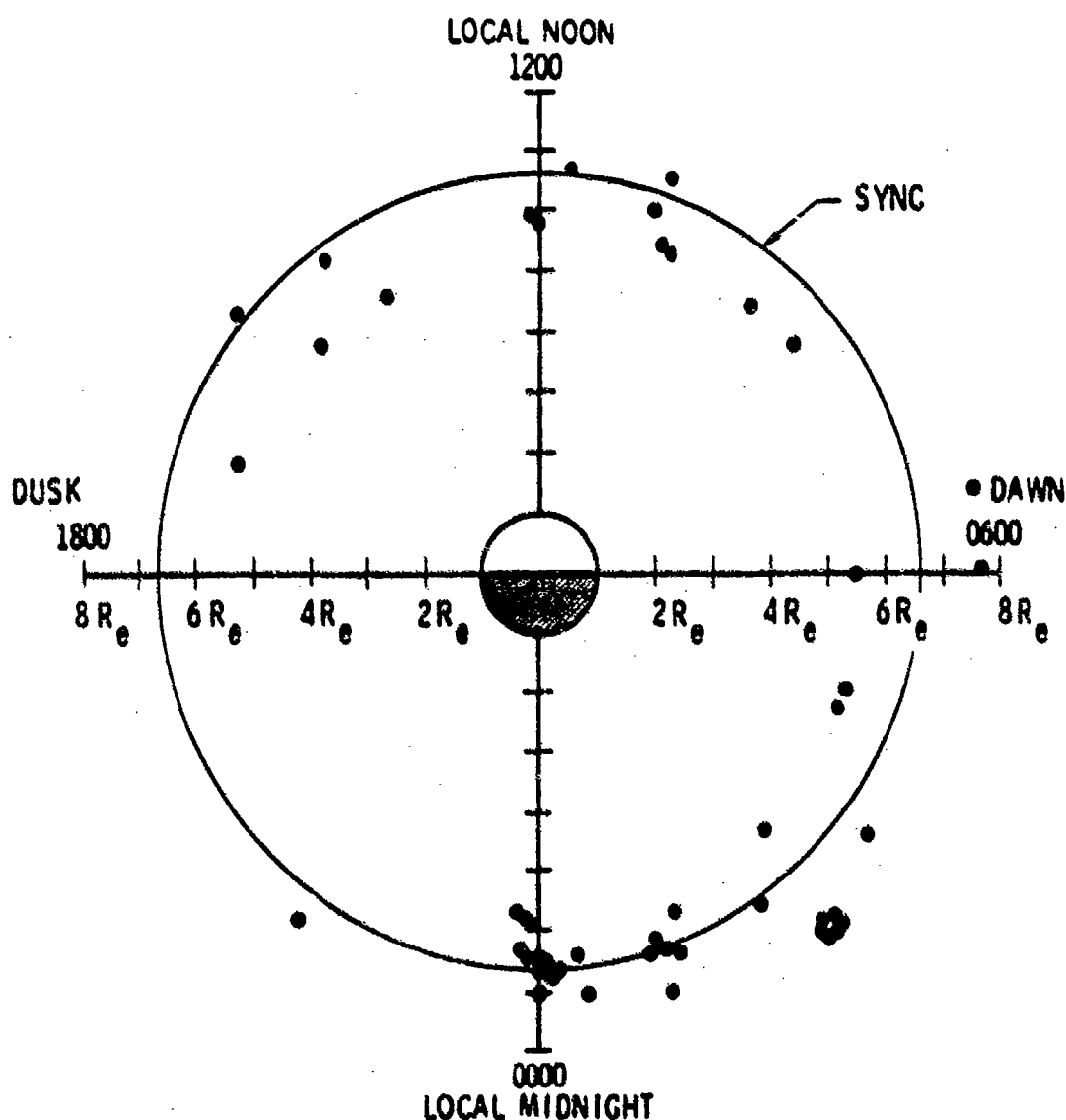

Figure 17. Local-time vs altitude plot of natural discharges observed by the Pulse Analyzer on the P78-2 satellite.

Figure 18 is a plot similar to Figure 17 except that the data are the pulses detected by the Transient Pulse Monitor and the data base covers only the 1979 time period. The Pulse Analyzer data set includes only one pulse during this time period that was thought to be due to bulk charging. The TPM data set shows a good correlation with regions of high probability for surface charging.
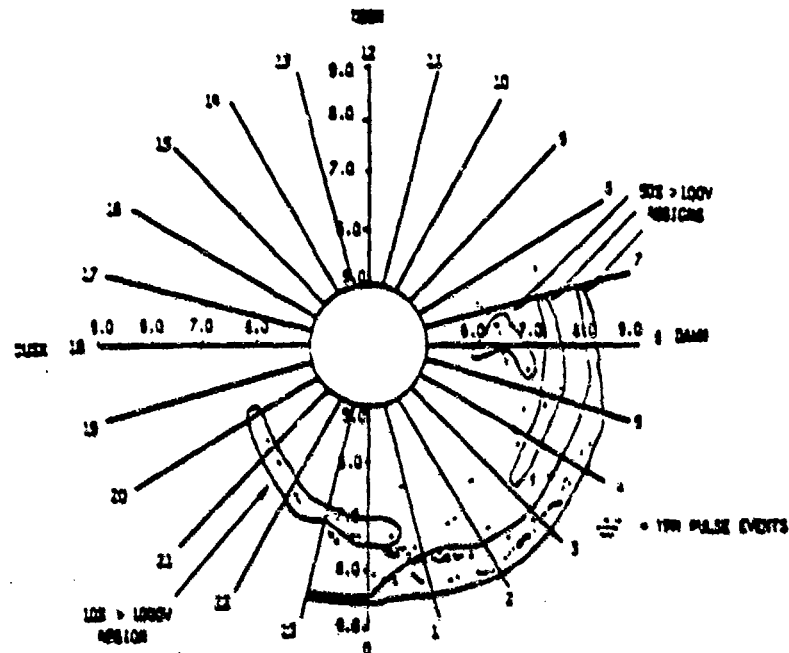

Figure 18. Altitude vs local-time plot of pulses detected by the Transient Pulse Monitor on P78-2 during 1979. Contours of surface charging probability from the SSPM are also indicated.

Electrostatic Fundamentals

An electrostatic potential is associated with every point in space. It is the energy required to move a test charge from infinity to the point. When the region contains a gas of charged particles (a plasma), this potential is called the 'plasma potential'. The potential of the undisturbed plasma in the vicinity of a spacecraft is a convenient reference for discussion of spacecraft surface charging.

When an object is immersed in a plasma and the surfaces are maintained at a potential other than the plasma potential, a region of disturbed plasma, called a sheath, is created. Unlike the undisturbed plasma, the average value of electric field strength is non-zero within a plasma sheath. Figure 19 shows a potential diagram for the case of a conductive sphere immersed in an idealized plasma. The physics of spacecraft immersed in the plasma of space is complicated by such effects as photo- and secondary-emission from the spacecraft, magnetic fields, non-uniformity of surface potential, non-spherical spacecraft shape, non-equilibrium and anisotropic plasma properties, departures from Maxwellian energy distributions, and the relative velocity between the spacecraft and the plasma. The sheath thickness decreases with plasma density and increases with vehicle surface potential and plasma temperature. At geosynchronous orbit altitude it can reach about 100 meters.
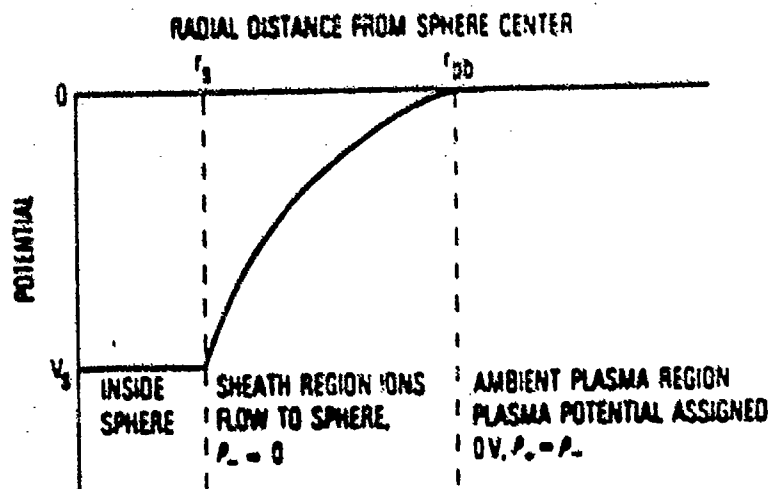

Figure 19. Potential diagram of a stationary conductive sphere immersed in an ideal plasma.

Contamination Considerations

Contamination collected on orbit by exterior surfaces of spacecraft originates from the spacecraft itself. At geosynchronous altitudes, a molecule usually follows a linear path between the points of release and interception. However, most of these large organic molecules escape from the vehicle with thermal velocity and therefore have a significant probability of ionization while still within the sheath. Ions created in the sheath can be re-attracted to the vehicle and strike surfaces having no view factor with the point of escape, thereby increasing the contamination rate of these surfaces. The point of each molecular impact will be determined by the 'ion optics' of the molecule--its velocity and position and the direction and magnitude of the electric field along its subsequent path.

Large surfaces which are the most negative on the spacecraft are most likely to attract contamination ions because they produce strong electric fields in a large volume of the sheath. It follows that if such surfaces are sensitive to contamination, such as fused quartz mirror radiators, surface charging reduction techniques will reduce contamination of the surfaces. If contamination-sensitive negative surfaces are small in area, it may be feasible to place biased electrodes nearby to deflect ionized contaminants.

Possible methods to control surface charging of dielectrics with respect to frame and other surface potentials include the use of transparent conductive films grounded to the vehicle frame, use of a lower resistivity dielectric together with a conductive adhesive mounting system, and development of dielectrics with more favorable secondary emission characteristics. Charging of the vehicle frame with respect to the plasma potential can be controlled with electron emitting devices and at least sometimes by having a sufficiently large photoemitting surface exposed to sunlight. Each of these techniques has disadvantages, but advantages may outweigh disadvantages in particular applications. For instance, indium-oxide, the most widely considered conductive coating, is expensive and apparently contributes to the increase in solar absorptance of materials during the first few months on orbit (Hall, 1983). However, these costs may be acceptable because of increased system life. It should be recognized that limiting vehicle frame charging will probably increase the differential potential between the frame and any exterior dielectric surface. The increased electric field may lead to more frequent or more intense discharges.

Effect of Charging on Contamination

The P78-2 satellite experiment complement included a Temperature Controlled Quartz Crystal Microbalance (Hall, 1975) which was designed to measure the rate of deposition of contaminants on satellite surfaces. The TQCM included a grid upon which a voltage could be imposed to repel ions. The mass detector was situated at the center of a 45 cm conductive plane at frame potential. Glass-covered solar cells bordered the plane. Long-term average mass accumulation rates over the four periods studied ranged from 0 to 31% greater when 0 to 500 eV ions were allowed to reach the mass detector than when they were reflected (Hall and Wakimoto, 1984). Figure 20 shows the effect of rejecting charged ions on the mass accumulation rate during one of the periods studied (Clark and Hall, 1981).
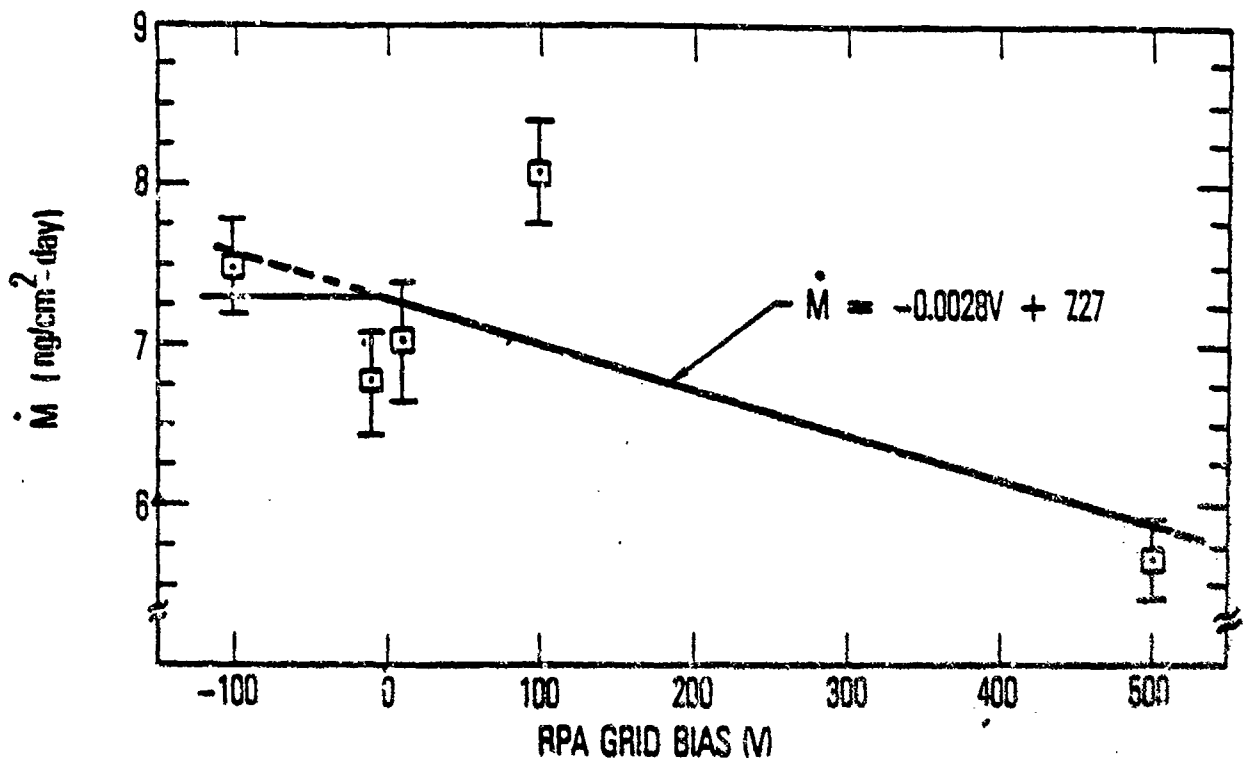

Figure 20. Mass accumulation rates on the P78-2 satellite as a function of repelling grid potential.

Surface Charging

Employ techniques to reduce electrical stress across dielectrics such as using electrically 'leaky' dielectrics or conductively-coated dielectrics. Coatings and the back surface of 'leaky' dielectrics should be grounded to the vehicle frame.

Time constants of electrical potential changes are as important as material properties in producing large differential potentials. Laboratory tests should give consideration to these time constants, including that of the vehicle frame.

Optical solar reflector tiles and solar cells should be bonded with conductive epoxy (or equivalent) to maintain surface potentials near frame potential.

Keep dielectrics away from surface-mounted sensors which are sensitive to discharges, electrical potentials, or contamination.

Spacecraft materials should be tested under a proper simulation of the space environment before inferring their electrical and thermal properties in space.

Computer simulations of charging (such as NASCAP) should be validated with realistic laboratory tests.

Properly designed and calibrated potential monitors can be valuable in assessing the operation of vehicles in geosynchronous orbit, especially in the event that anomalous operation occurs.

P78-2 experience indicates that attempts to control frame potential with charged-particle beams aggravates differential charging. A more complete understanding of the physics of particle beams in plasmas is required before their utility on operational vehicles can be determined.

Bulk Charging

Bulk charging can be reduced by reducing the flux of energetic electrons which can reach critical dielectrics in cables and circuit boards. Keep all cables and circuit boards within the body of the satellite when practical.

Use a minimum of 35 mils of aluminum (or equivalent mass) between the dielectric and the space environment.

Large areas of metallization on circuit boards should be grounded. All conductors in cables should be terminated at both ends, even if unused.

Design circuits to be insensitive to the type of pulse generated by bulk dielectric discharges. Avoid using input elements with a low damage threshold. Use circuit and structure designs which minimize coupling of discharge energy into circuits.

Discharges

Discharges occur when metal surfaces separated by a dielectric become charged to different potentials. To prevent this, use adequate electrical bonding between metal sections to keep all metal parts at approximately the same potential. Streamer discharges can also occur on dielectric materials from the nonmetallic areas to the adjacent metal when each is charged to a different potential. Streamering may be overcome by shielding the nonmetallic areas with electrically-conducting coatings that will keep the surfaces at approximately the same potential. Examples include indium-oxide coatings on solar cells, conductive paints, and metallized Kapton with the metallic side out. These coatings must be electrically grounded to the vehicle frame.

All wiring should be routed within the spacecraft metallic structure (skin) or shielded. The skin should be as continuous as practical to provide as good a Faraday cage as practical. Note that some electromagnetic fields will enter the vehicle, either by propagation through the skin or by direct penetration through apertures such as seams, grids, nonmetallic sections, antennas, and external wiring harnesses.

Establish upset criteria for all circuits. Protect all circuits that may be damaged or upset by short duration current or voltage spikes. Consider proper equipment and circuit design, shielding, decoupling, filters, good mechanical layout, and proper parts placement in all solid state applications.

Testing of full scale samples in exact production configuration is advisable when the safety of the vehicle is involved.

48

Contamination

Reduction of the potential of the vehicle, or parts of the vehicle near sensitive surfaces, will reduce the rate of contamination.

References

Cauffman, D. P., "Ionization and Attraction of Neutral Molecules to a Charged Spacecraft," AFSD Rept. No. SD-TR-80-78, December 1980.

Clark, D. M. and D. F. Hall, "Flight Evidence of Spacecraft Surface Contamination Rate Enhancement by Spacecraft Charging Obtained with a Quartz-Crystal Microbalance," Proc. of 3rd AF/NASA Spacecraft Charging Technology Conference, NASA Conf. Pub. CP 2182, 493, 1981.

DeForest, S. E., "Spacecraft Charging at Synchronous Orbit," J. Geophys. Res., 77, 651, 1972.

Feuerbacher, B. and B. Fitton, "Experimental Investigation of Photoemission from Satellite Surface Materials," J. Appl. Phys., 43, 1563, 1972.

Fredricks, R. W. and F. L. Scarf, "Observations of Spacecraft Charging Effects in Energetic Plasma Regions," Photon and Particle Interactions with Surfaces in Space, D. Reidel, Dordrecht, Holland, 271, 1973.

Garrett, H. B., "The Charging of Spacecraft Surfaces," Rev. Geophys. Space Phys., 19, 577, 1981.

Grard, R. J. L., K. Knott and A. Pederson, "The Influences of Photoelectrons and Secondary Emission on Electric Field Measurements in the Magnetosphere and Solar Wind," IBID, 163, 1973.

Grard, R. J. L., "Properties of the Satellite Photoelectron Sheath Derived from Photoemission Laboratory Measurements," J. Geophys. Res., 78, 2885, 1973.

Hall, D. F., "Experiment to Measure Enhancement of Spacecraft Contamination by Spacecraft Charging," NASA SP-379, National Technical Information Service, 1975.

Hall, D. F. and A. A. Fote, "α_s/ϵ_H Measurements of Thermal Control Coatings Over Four Years at Geosynchronous Altitude," AIAA-83-1450, June 1983.

Hall, D. F. and J. N. Wakimoto, "Further Flight Evidence of Spacecraft Surface Contamination Rate Enhancement by Spacecraft Charging," AIAA-84-1703, June 1984.

Katz, I., J. J. Cassidy, M. J. Mandell, G. W. Schnuelle, P. B. Steen, D. E. Parker, M. Rotenburg and J. H. Alexander, "Extension, Validation and Application of the NASCAP Code," NASA, CR-159595, January 1979.

Koons, H. C., "Summary of Environmentally Induced Electrical Discharges on the P78-2 (SCATHA) Satellite, AIAA-82-0264, Orlando, Florida, January 1982.

Leung, M. S., P. F. Mizera and R. M. Broussard, "Space Effects on Physical Properties of Materials," ATR-82(8378)-1, The Aerospace Corporation, 1982.

Mizera, P. F., H. C. Koons, E. R. Schnauss, D. R. Croley, Jr., H. K. A. Kan, M. S. Leung, N. J. Stevens, F. Berkopec, J. Staskus, W. L. Lehn and J. Nanewicz, "First Results of Material Charging in the Space Environment, App. Phys. Lett., 37, 276, 1980.

Mizera, P. F., J. F. Fennell, H. C. Koons and D. Hall, "Spacecraft Charging in the Spring of 1981," TOR-0081(6508-05)-1, The Aerospace Corporation, 1981.

Mizera, P. F., "A Summary of Spacecraft Charging Results," J. Spacecraft and Rockets, in press, 1983.

Mullen, E. G., M. S. Gussenhoven and H. B. Garrett, "A 'Worst Case' Spacecraft Charging Environment as Observed by SCATHA on 24 April 1979," AFGL-TR-81-0231, ADA108680, 1981.

Mullen, E. G. and M. S. Gussenhoven, "SCATHA Environmental Atlas," AFGL-TR-83-0002, 75, 3 January 1983.

Reagan, J. B., R. E. Meyerott, E. E. Gaines, R. W. Nightingale, P. C. Filbert and W. L. Imhof, "Space Charging Currents and their Effects on Spacecraft Systems," Proc. 10th International Symposium on Discharges and Electrical Insulation in Vacuum, October 1982.

LABORATORY OPERATIONS

The Laboratory Operations of The Aerospace Corporation is conducting
experimental and theoretical investigations necessary for the evaluation and
application of scientific advances to new military space systems. Versatility
and flexibility have been developed to a high degree by the laboratory person-
nel in dealing with the many problems encountered in the nation's rapidly
developing space systems. Expertise in the latest scientific developments is
vital to the accomplishment of tasks related to these problems. The labora-
tories that contribute to this research are:

Aerophysics Laboratory: Launch vehicle and reentry fluid mechanics, heat
transfer and flight dynamics; chemical and electric propulsion, propellant
chemistry, environmental hazards, trace detection; spacecraft structural
mechanics, contamination, thermal and structural control; high temperature
thermomechanics, gas kinetics and radiation; cw and pulsed laser development
including chemical kinetics, spectroscopy, optical resonators, beam control,
atmospheric propagation, laser effects and countermeasures.

Chemistry and Physics Laboratory: Atmospheric chemical reactions, atmo-
spheric optics, light scattering, state-specific chemical reactions and radia-
tion transport in rocket plumes, applied laser spectroscopy, laser chemistry,
laser optoelectronics, solar cell physics, battery electrochemistry, space
vacuum and radiation effects on materials, lubrication and surface phenomena,
thermionic emission, photosensitive materials and detectors, atomic frequency
standards, and environmental chemistry.

Computer Science Laboratory: Program verification, program translation,
performance-sensitive system design, distributed architectures for spaceborne
computers, fault-tolerant computer systems, artificial intelligence and
microelectronics applications.

Electronics Research Laboratory: Microelectronics, GaAs low noise and
power devices, semiconductor lasers, electromagnetic and optical propagation
phenomena, quantum electronics, laser communications, lidar, and electro-
optics; communication sciences, applied electronics, semiconductor crystal and
device physics, radiometric imaging; millimeter wave, microwave technology,
and RF systems research.

Materials Sciences Laboratory: Development of new materials: metal
matrix composites, polymers, and new forms of carbon; nondestructive evalua-
tion, component failure analysis and reliability; fracture mechanics and
stress corrosion; analysis and evaluation of materials at cryogenic and
elevated temperatures as well as in space and enemy-induced environments.

Space Sciences Laboratory: Magnetospheric, auroral and cosmic ray phys-
ics, wave-particle interactions, magnetospheric plasma waves; atmospheric and
ionospheric physics, density and composition of the upper atmosphere, remote
sensing using atmospheric radiation; solar physics, infrared astronomy,
infrared signature analysis; effects of solar activity, magnetic storms and
nuclear explosions on the earth's atmosphere, ionosphere and magnetosphere;
effects of electromagnetic and particulate radiations on space systems; space
instrumentation.

. . .